Preprints of the 19th World Congress
The International Federation of Automatic Control
Cape Town, South Africa. August 24-29, 2014

$\mathcal{L}_1$ Adaptive Control Design for Hysteresis Compensation within Piezoelectric Actuators

Jie Zhang*. Qinmin Yang*. Chunlin Zhou*

**State Key Laboratory of Industrial Control Technology,*
Department of Control Science and Engineering, Zhejiang University,
Hangzhou, Zhejiang 310027 China, (e-mail: qmyang@zju.edu.cn)

Abstract: Hysteresis nonlinearity of piezoelectric actuator deteriorates its control performance. Unlike traditional model-based control scheme, this paper employs a novel $\mathcal{L}_1$ adaptive control algorithm without modeling of hysteresis to achieve a precise tracking control. The piezoelectric actuator system in question consists of models in the form of a linear time-invariant dynamic system in series with a differential hysteresis model. The hysteresis can be transformed into general uncertainties to the system. Then an $\mathcal{L}_1$ adaptive control algorithm can be applied. By implementing this control scheme on the piezoelectric actuator system and comparing its result to the result of a PID controller, the effectiveness of this controller is verified.

Keywords: Nano-positioning, Piezoelectric actuators, Hysteresis, $\mathcal{L}_1$ adaptive control, Tracking control

1. INTRODUCTION

Since the discovery of piezoelectric effect and converse piezoelectric effect, piezoelectric actuators made of ceramic materials have been widely used in numerous applications, such as precision mechanics, data storage optics, life science, medical technology and so on (Li, and Xu, 2010). However, the applicability of piezoelectric actuators are still severely constrained due to the existence of hysteresis, creep, thermal drift and other forms of nonlinearity, among which hysteresis is the most undesirable behavior. It is reported that the maximum error caused by hysteresis nonlinearity can be as much as 10-15% of the trajectory covered when the piezoelectric actuators run in an open loop manner (Physik Instrumente, 2009).

To attain better dynamic performance of piezoelectric actuators, many efforts have been made recently from multiple perspectives. Generally speaking, the existing schemes can be grouped into two categories (Ge, and Jouaneh, 1996):

(a). Utilization of electric charge to drive piezoelectric actuators instead of applied voltage (Fleming, and Moheimani, 2005).

(b). Model-based closed-loop control schemes.

The first class of approaches is highly limited by the requirement of a specially designed charge/current amplifier to drive highly capacitive loads. Therefore, implementation of advanced control law is commonly believed to be a promising and economical solution to such a problem.

In that effort, various methods have been introduced to model hysteresis phenomenon, including Bouc-Wen model, Maxwell resistive capacitor model, Prandtl-Ishlinkii model (Chen, Qiu, 2013), Preisach model (Song, Zhao, and Zhou, 2005), neural network model (Li, and Tan, 2004), and so on. Preisach model and its extensions are most popularly adopted because of its ability to approximate complex hysteresis loops. It is a summation of an amount of basic Presiach operators with two thresholds, which unfortunately makes it difficult to achieve an accurate expression of its inverse model. In addition, the parameters of Preisach model have to be updated along with the changes of time, frequency and amplitude of driving voltage. Thus, the complexity of Preisach model based control algorithms will be further increased when the operating conditions are varying.

For applications that require broadband compensation, a form of decoupled linear sub-system with nonlinear hysteresis as input is adopted to capture the dynamics, while the nonlinear hysteresis is modeled in the hysteresis sub-system (Banning, de Koning, Adriaens, and Richard, 2001). Based on this decouple system, a few theoretical works have been proposed to deal with unknown hysteresis dynamics by using intelligent control laws (Fan, and Smith, 2008). However, their applicability on an actual piezoelectric transducer (PZT) based actuator has not been verified.

Therefore, a novel $\mathcal{L}_1$ adaptive control algorithm, which was originally proposed in (Cao, and Hovakimyan, 2006), is investigated to accommodate the hysteresis effect without explicitly modeling its dynamics. Thus, compared with traditional model-based approaches, constructing an accurate mathematical model of sophisticated hysteresis phenomenon is relaxed. To verify the feasibility of our scheme, it is implemented on an actual PZT motion platform and compared with traditional PID controller. Experimental results demonstrate that the proposed method is able to achieve a satisfactory tracking performance under different working conditions.

Copyright © 2014 IFAC

In the second section, we formulate the control problem based on a series of experiments on the PZT actuator system. Then, the $\mathcal{L}_1$ adaptive controller design is specified. Subsequently, the experimental results are obtained. Finally, the paper is concluded with some remarks.

2. PROBLEM FORMULATION

2.1 State-space representation

To capture the dynamics of piezoelectric systems, a model consisting of a hysteretic unit and a linear system has been developed as shown in Fig.1 (Devasia, and Moheimani, 2007). The input u is the applied driving voltage on the piezoelectric actuator, while y is its displacement, and ω is an intermediate variable denoting the output of the hysteresis sub-model. This model structure has been widely utilized for tracking controller designs in literatures (de Koning, Adriaens, and Banning, 1998).

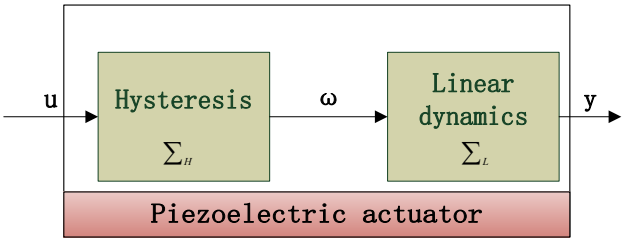

Fig.1 A typical decoupled model of piezoelectric actuators

The hysteresis subsystem Σ_H is commonly modeled as a nonlinear time-varying function of the input u, such that

$$\Sigma_H \triangleq \omega(t) = \varphi(u(t), t) \tag{1}$$

Besides, the dynamic behavior of a one-dimensional piezoelectric actuator can be represented by a second order damped mass-spring-system (Banning, Koning, & Adriaens, 2001). Ideally, it can be given as

$$\ddot{y}(t) + \alpha\dot{y}(t) + \beta y(t) = \varepsilon\omega(t) \tag{2}$$

or in state-space controllability canonical form

$$\Sigma_L \triangleq \begin{cases} \dot{x}(t) = Ax(t) + B\omega(t) \\ y(t) = Cx(t) \end{cases} \tag{3}$$

where $A = \begin{bmatrix} 0 & 1 \\ -\beta & -\alpha \end{bmatrix}$, $B = \begin{bmatrix} 0 \\ \varepsilon \end{bmatrix}$, $C = [1 \quad 0]$. $x(t) = [y(t) \ \dot{y}(t)]^T$ and α, β, ε are unknown positive parameters. Meanwhile, $x(0) = [y(0) \ \dot{y}(0)]^T$ and $y(0) = y_0$ denote the initial condition of the piezoelectric actuator.

Moreover, if an additive time-varying disturbance $\sigma_0(t)$ is taken into account of the system, the overall system can be given as

$$\Sigma_o \triangleq \begin{cases} \dot{x}(t) = Ax(t) + B(\omega(t) + \sigma_0(t)) \\ y(t) = Cx(t) \end{cases} \tag{5}$$

$\sigma_0(t)$ usually contains the environmental noise and external disturbances. It can be reasonably assumed to be bounded by $|\sigma_0(t)| \leq \Omega$.

Then, the control objective is to design a feedback adaptive controller $u(t)$ to ensure that the output $y(t)$ tracks the output of a desired system

$$\begin{cases} \dot{x}_{des}(t) = A_m x_{des}(t) + Bk_g r(t) \\ y_{des} = Cx_{des}(t) \end{cases} \tag{6}$$

with satisfactory steady state and transient performance. A_m is specified by users, which determines the system dynamic response. $r(t)$ is a bounded reference input, which is usually given a priori.

Thus, the overall system (5) can be rewritten as following:

$$\begin{cases} \dot{x}(t) = A_m x(t) + B(\varphi(u(t), t) + \theta^T x(t) + \sigma_0(t)) \\ y(t) = Cx(t) \end{cases} \tag{7}$$

where $B\theta^T x(t)$ represents the difference between $Ax(t)$ within actual system and $A_m x(t)$ within desired system, i.e. $A = A_m + B\theta^T$ with $A_m = \begin{bmatrix} 0 & 1 \\ -\beta_0 & -\alpha_0 \end{bmatrix}$. Apparently, θ is also an unknown parameter.

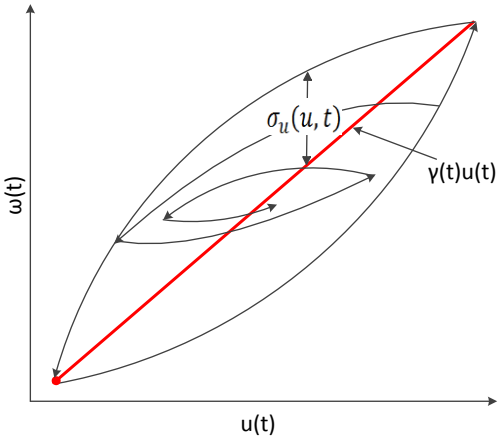

Fig.2 Relation between ω(t) and γ(t)u(t)

2.2 Hysteresis transformation

As a matter of fact, system (7) can be seen as a nonaffine system with unknown dynamics, which poses a challenge to controller design. Alternatively, recalling the trajectories of hysteresis loop $\omega(t)$ shown in Fig.2, it has been proven that for any bounded input $u(t)$, we can always find bounded $\gamma(t)$ and $\sigma_u(t)$ such that (Zou, Luo, and Cao, 2013):

$$\omega(t) = \gamma(t)u(t) + \sigma_u(u, t) \tag{8}$$

where $\gamma(t)$ is a time-varying parameter satisfying $\gamma_l < \gamma(t) < \gamma_u$ with $0 < \gamma_l < \gamma_u \leq d_\gamma$, and d_γ being a positive constant. $\sigma_u(u, t)$ has the following properties:

(a) $|\sigma_u(u,t)| < \sigma_b < \infty$
(b) $\sigma_u(u,t)$ is piece-wise differentiable with respect to u
(c) If $\dot{u}$ is bounded, then $\dot{\sigma}_u(u,t)$ is also bounded although $\dot{\sigma}_u(u,t)$ is discontinuous.

Therefore, the original system (7) can be transformed into:

$$\begin{cases}\dot{x}(t) = A_m x(t) + B\big(\gamma(t)u(t) + \theta^T(t)x(t) + \sigma(u,t)\big) \\ y(t) = Cx(t)\end{cases} \tag{9}$$

where $\sigma(u,t) = \sigma_0(t) + \sigma_u(u,t)$, which is subject to:

$$\begin{cases}|\sigma(u,t)| \le \Delta \\ \Delta = \sigma_b + \Omega\end{cases} \tag{10}$$

3. $\mathcal{L}_1$ ADAPTIVE CONTROLLER

In this section, an $\mathcal{L}_1$ adaptive control based scheme is introduced for tracking task of PZT actuators in the present of unknown hysteresis. The objective of the controller is to drive the actuator displacement $y(t)$ to follow a bounded reference signal $r(t)$ with satisfactory transient and steady state performance.

3.1 Architecture of $\mathcal{L}_1$ adaptive controller

The architecture of $\mathcal{L}_1$ adaptive controller proposed in this work can be shown in Fig.3, which consists of three components:

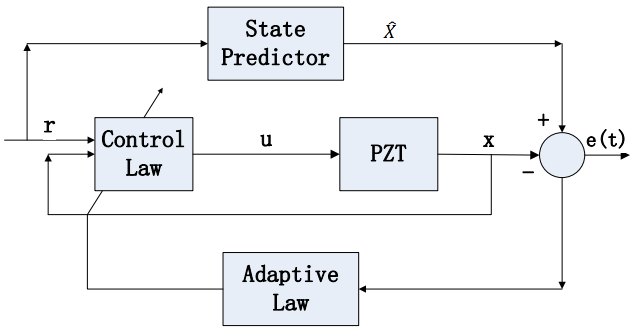

Fig.3 Architecture of $\mathcal{L}_1$ adaptive controller

(1) State Predictor:

$$\begin{cases}\dot{\hat{x}}(t) = A_m x(t) + B(\hat{\gamma}(t)u(t) + \hat{\theta}^T x(t) + \hat{\sigma}(t)) \\ \hat{y}(t) = C\hat{x}(t), \quad \hat{x}(0) = x_0\end{cases} \tag{11}$$

The state predictor has the same structure as the system given in (9). The unknown parameters $\theta(t)$, $\sigma(u,t)$, $\gamma(t)$ are replaced by their estimates $\hat{\theta}(t)$, $\hat{\sigma}(u,t)$, $\hat{\gamma}(t)$ respectively, which are governed by following adaptive laws.

(2) Adaptive Laws:

$$\begin{cases}\dot{\hat{\theta}}(t) = -\Gamma e(t)^T PB, & \hat{\theta}(0) = \theta_0 \\ \dot{\hat{\sigma}}(t) = -\Gamma e(t)^T PBx(t), & \hat{\sigma}(0) = \sigma_0 \\ \dot{\hat{\gamma}}(t) = -\Gamma e(t)^T PBu(t), & \hat{\gamma}(0) = \gamma_0\end{cases} \tag{12}$$

where $e(t) = \hat{x}(t) - x(t)$, and $P = P^T > 0$ is the solution of the algebraic equation $A_m^T P + P^T A_m = -Q(Q > 0)$. The adaption rate Γ is a user specified positive constant. $\theta_0, \sigma_0, \gamma_0$ are initial values of $\theta(t), \sigma(u,t), \gamma(t)$ respectively, and they can be conveniently set as 0.

(3) Control Law:

$$\begin{cases}\dot{\chi}(t) = \hat{\gamma}(t)u(t) + \hat{\theta}^T x(t) + \hat{\sigma}(t) - k_g r(t) \\ u(t) = -k\chi(t)\end{cases} \tag{13}$$

with $k_g = -1/(CA_mB)$ being a constant and k a positive constant.

3.2 Stability analysis

By assuming that all parameters of the system are known, a closed-loop reference system is firstly constructed as following to assist the stability analysis of the original system:

$$\begin{cases}\dot{x}_{ref}(t) = A_m x_{ref}(t) + B(\gamma(t)u_{ref}(t) + \theta^T(t)x_{ref}(t) \\ \qquad\qquad +\sigma(u,t)) \\ \dot{\chi}_{ref}(t) = \gamma(t)u_{ref}(t) + \theta^T(t)x_{ref}(t) + \sigma(u,t) - k_g r(t) \\ u_{ref}(t) = -k\chi_{ref}(t) \\ y_{ref}(t) = Cx_{ref} \\ x_{ref}(0) = x_0 \\ u_{ref}(0) = u_0\end{cases} \tag{14}$$

Consider the equations of $\chi(t)$ and $u_{ref}(t)$ in (14), whose analytical solution is

$$u_{ref}(t) = e^{-\int_0^t k\gamma(\tau)d\tau}\{u_0 + \int_0^t k[g_1(\tau) - g_2(\tau)]e^{\int_0^\tau k\gamma(s)ds}\,d\tau\} \tag{15}$$

with

$$\begin{cases}g_1(t) = k_g r(t) \\ g_2(t) = \theta^T(t)x_{ref}(t) + \sigma(u,t)\end{cases} \tag{16}$$

Then we define following systems as:

$$\mathrm{H}: \begin{cases}\dot{x}_{ref}(t) = A_m x_{ref}(t) + Bh \\ y_{ref}(t) = Cx_{ref}, \quad x_{ref}(0) = x_0 \\ h = \theta^T(t)x_{ref}(t) + \sigma(u,t) + \gamma(t)u_{ref}(t)\end{cases} \tag{17}$$

$$C_1: \begin{cases}\dot{x}_1(t) = -k\gamma(t)x_1(t) + kg_1(t) \\ h_1 = \gamma(t)x_1(t)\end{cases} \tag{18}$$

$$C_2: \begin{cases}\dot{x}_2(t) = -k\gamma(t)x_2(t) + kg_2(t) \\ h_2 = g_2(t) - \gamma(t)x_2(t)\end{cases} \tag{19}$$

Meanwhile, HC_1 and HC_2 are defined as cascaded systems of (H, C_1) and (H, C_2) respectively.

Then we can obtain that

$$h_1 = \gamma(t)e^{-\int_0^t k\gamma(\tau)d\tau}\{c_1(0) + \int_0^t kg_1(\tau)e^{\int_0^\tau k\gamma(s)ds}\,d\tau\} \tag{20}$$

$$h_2 = g_2(t) - \gamma(t)e^{-\int_0^t k\gamma(\tau)d\tau}\left\{c_2(0) + \int_0^t kg_2(\tau)e^{\int_0^\tau k\gamma(s)ds}\,d\tau\right\} \tag{21}$$

By setting $c_1(0) - c_2(0) = u_0$, combining (15) (16) (20) (21) delivers

$$h_1 + h_2 = \theta^T(t)x_{ref}(t) + \sigma(u,t) + \gamma(t)u_{ref}(t) \tag{22}$$

So the closed-loop reference system can be depicted as in Fig. 4. Since system H, C_1, C_2 can be seen as time-varying linear system, one has,

$$x_{ref}(t) = (HC_1)\{g_1\} + (HC_2)\{g_2\} + h_0 \quad (23)$$

where $h_0 = (sI - A_m)^{-1}x_0$.

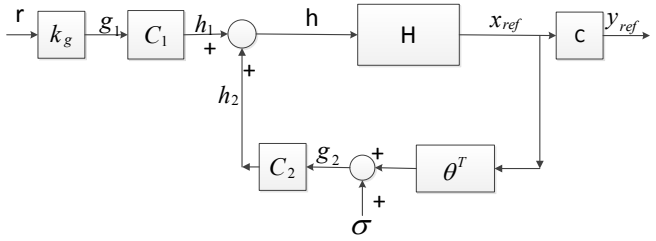

Fig.4 Diagram of the closed-loop reference system

(23) directly gives that

$$\|x_{ref}\|_\infty \le \|HC_1\|_1\|g_1\|_\infty + \|HC_2\|_1\|g_2\|_\infty + \|h_0\|_\infty \quad (24)$$

$$\|g_1\|_\infty = \|k_g r(t)\|_\infty \quad (25)$$

$$\|g_2\|_\infty \le \|\theta^T(t)x_{ref}(t)\|_\infty + \Delta \le \|\theta^T\|_\infty\|x_{ref}\|_\infty + \Delta \quad (26)$$

Throughout this paper, $\|H\|_1$ denotes the $\mathcal{L}_1$ norm of $H(s)$, and $\|x\|_\infty$ denotes the ∞-norm of variable $x(t)$ respectively. With the help of (24)-(26), we are able to derive that

$$\|x_{ref}\|_\infty \le \|HC_1\|_1\|g_1\|_\infty + \|HC_2\|_1\{\|\theta^T\|_\infty\|x_{ref}\|_\infty + \Delta\} + \|h_0\|_\infty \quad (27)$$

The initial state of the system x_0 is 0 in general. Meanwhile, since θ^T is bounded, and H, C_2 are user designed, the following inequalities are able to be satisfied:

$$\|x_0\|_\infty < \rho_x \quad (28)$$

$$\|HC_2\|_1\|\theta^T\|_\infty < 1 \quad (29)$$

with ρ_x being a positive constant defined later. Equation (27) can be further rewritten as

$$\|x_{ref}\|_\infty \le \rho_x \quad (30)$$

$$\rho_x = \frac{\|HC_1\|_1\|g_1\|_\infty + \|HC_2\|_1\Delta + \|h_0\|_\infty}{1 - \|HC_2\|_1\|\theta^T\|_\infty}$$

If follows from (22) and (16) that

$$u_{ref} = \frac{h_1 + h_2 - g_2}{\gamma(t)} \quad (31)$$

where $h_1 = C_1\{g_1\}$, $h_2 = C_2\{g_2\}$, $\gamma_l < \gamma(t) < \gamma_u$. Therefore, by referring to (25)-(30), we have

$$\|u_{ref}\|_\infty \le \rho_u \quad (32)$$

$$\rho_u = \frac{\|C_1\|_1\|g_1\|_\infty + (\|C_2\|_1 + 1)(\|\theta^T\|_\infty\rho_x + \Delta)}{\gamma_l}$$

So we are able to conclude that the control input u_{ref} and state x_{ref} of the reference system are bounded. Moreover, considering equation (22), we have

$$\gamma(t)u_{ref}(t) + \theta^T(t)x_{ref}(t) + \sigma = (C_1)\{g_1\} + (C_2)\{g_2\} \quad (33)$$

When k is large enough, $(C_1)\{g_1\} \approx k_g r(t)$, $(C_2)\{g_2\} \approx 0$,

$$\dot{x}_{ref}(t) \approx A_m x_{ref}(t) + Bk_g r(t) \quad (34)$$

Hence the response of the reference system can approximate the desired system (6) with certain quantifiable performance.

Subsequently, following theorem is given to show that the response of the closed-loop adaptive system can be rendered arbitrarily close to that of the reference system in the presence of fast adaption.

Theorem 1: Consider the reference system and the closed-loop $\mathcal{L}_1$ adaptive controller subject to (31), if $\|x_0\|_\infty$ is bounded and the adaption rate is chosen to verify a lower bound $\Gamma > \Gamma_0$, we have:

$$\begin{cases} \|x - x_{ref}\|_\infty < \rho_3 \\ \|u - u_{ref}\|_\infty < \rho_4 \end{cases} \quad (35)$$

ρ_3, ρ_4 are positive parameters defined as follows:

$$\rho_3 = \frac{\|HC_1\frac{1}{CH}C\|_1}{1 - \|HC_2\|_1\|\theta^T\|_\infty}\rho_0 + \rho_1 \quad (36)$$

$$\rho_4 = \frac{\|\theta^T\|_\infty}{\gamma(t)}\|C_1\|_1\rho_3 + \frac{1}{\gamma_l}\left\|C_1\frac{1}{CH}C\right\|_1\rho_0 \quad (37)$$

ρ_0, ρ_1 are arbitrarily small positive constants, and so are ρ_3, ρ_4. $C = [1\ 0]$ is defined in (3).

Proof: The proof is similar to that in (Zou, Luo, and Cao, 2013) and thus is omitted here.

With Theorem 1 and (34), we can reach the conclusion that the dynamic response of the original system can be made as close as demanded to that of the desired system. Thus, the performance of the closed-loop adaptive system can be completely characterized by the desired system (6).

Furthermore, combining (30), (32), and (36)-(37) yields

$$\begin{cases} \|x\|_\infty < \rho_x + \rho_3 \\ \|u\|_\infty < \rho_u + \rho_4 \end{cases} \quad (38)$$

which means that all signals are bounded within the closed-loop system.

4. EXPERIMENT

4.1 Experiment setup

The architecture of the experimental setup studied in this paper is demonstrated in Fig.5.

The piezoelectric actuator (model 20vs12 produced by Harbin Core Tomorrow & Technology Co. Ltd) has a stroke of 0-22um with driving voltage within 0-150v supplied by a voltage amplifier module (XE-501), which can linearly amplify a 0-10v voltage to 0-150v. The actuator has an integrated high-resolution strain gauge position sensor (SGS)

which can measure the displacement in a real-time manner. Equipped with the position sensing module (XE-509.S1 PZT), the displacement data are translated to voltage data and are in turn provided to the controller as a feedback signal for closed-loop operation. The control algorithms running on a personal computer are implemented by LabVIEW. A data acquisition card (PCI-1716 by ADVANTECH) with integrated AD and DA converter is utilized to convert the digital control output to 0-10v analog signal for amplification and convert analog displacement signal to digital signal for computer processing. The resolution of the AD converter is 16-bit, while that of the DA converter is 12-bit.

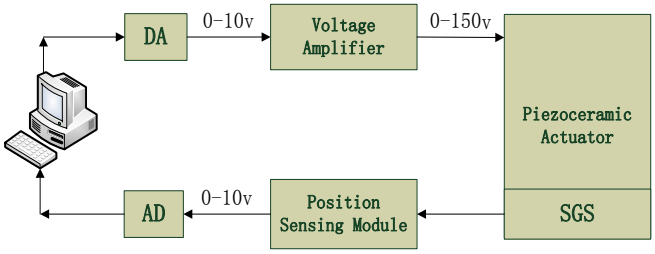

Fig.5 Diagram of our experiment setup

4.2 Controller Design

To verify the feasibility of our proposed scheme, the goal of our control is to maneuver the piezoelectric actuator to track a given trajectory. In other words, the displacement of the actuator $y(t)$ should follow a reference input signal $r(t)$ with satisfactory transient and steady state performance. In our experiment, the reference input signal $r(t)$ is chosen as a sinusoidal signal, with amplitude varying from 0-10v. The controller parameters are set as

$$A_m = \begin{bmatrix} 0 & 1 \\ -400 & -4 \end{bmatrix} \quad B = \begin{bmatrix} 0 \\ 400 \end{bmatrix} \quad C = [1 \;\; 0]$$

$$\Gamma = 1,\ k = 120,\ P = \begin{bmatrix} 0.1303 & -0.5 \\ -0.5 & 50.125 \end{bmatrix}$$

4.3 Experimental results

To test the performance of the $\mathcal{L}_1$ controller, it is implemented on our piezoelectric actuator positioning platform. For comparison purpose, a proportional integral derivative (PID) control algorithm is also implemented.

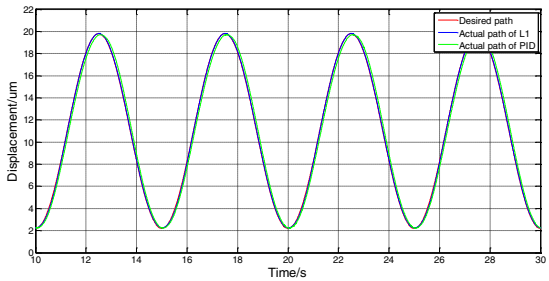

Fig.6.(a) Sinusoidal motion tracking trajectory of the piezoelectric actuator system with 0.2 Hz input frequency by using PID and $\mathcal{L}_1$ adaptive controller

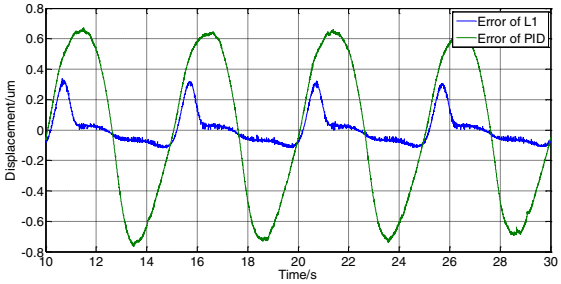

Fig.6.(b) Zoomed in tracking error of PID and $\mathcal{L}_1$ controller

Firstly, a 0.2Hz sinusoidal reference input is investigated to compare the tracking performance of PID controller and $\mathcal{L}_1$ controller. The obtained tracking result is demonstrated in Fig.6. In Fig.6(a), both the PID and $\mathcal{L}_1$ controller can track the desired trajectory. However, when the tracking error is zoomed-in and depicted in Fig.6(b), due to existence of unmodeled hysteresis effect, a recurrent tracking error is present, and evidently, $\mathcal{L}_1$ controller outperforms the PID counterpart in terms of error amplitude. Quantitatively, the maximum peak-to-peak (PP) tracking error produced by PID controller is calculated to be 1.438um and the root-mean-square error (RMS) is 0.492um, i.e., 6.53% and 2.23% of the motion range respectively. In contrast, the $\mathcal{L}_1$ controller produces a maximum peak-to-peak (PP) tracking error of 0.4553um and a root-mean-square error (RMS) of 0.1071um, which gives 2.06% and 0.48% of the total motion range respectively.

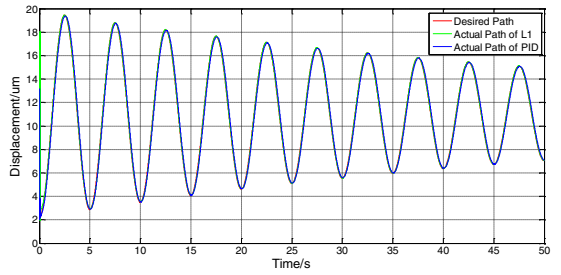

Fig.7.(a) Tracking trajectory of the piezoelectric actuator system with 0.2 Hz input frequency and varying amplitude by using PID and $\mathcal{L}_1$ adaptive controller

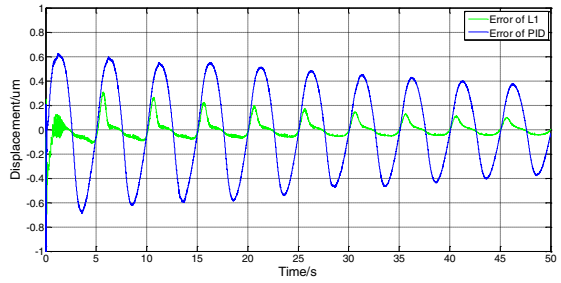

Fig.7.(b) Zoomed in tracking error of PID and $\mathcal{L}_1$ controller

Furthermore, the performance of the proposed controller is also testified by utilized a sinusoidal signal with a frequency of 0.2 Hz but varying amplitude. From the result shown in Fig.7(a) and (b), it is obvious that with the decreasing amplitude of the sinusoidal signal, the tracking error also descends, which is consistent with the property of hysteresis.

We can conclude that after a short transition period initially, both PID and $\mathcal{L}_1$ controller can track the desired path. However, $\mathcal{L}_1$ controller is able to be adapted to the varying conditions and achieve a lot smaller tracking error. Meanwhile, after the transition period, the maximum peak-to-peak (PP) tracking error produced by PID controller is 1.315um and the root-mean-square error (RMS) is 0.3768um, i.e., 5.97% and 1.71% of the motion range respectively. In contrast, the $\mathcal{L}_1$ controller produces a maximum peak-to-peak (PP) tracking error of 0.4178um and root-mean-square error (RMS) of 0.0689um, i.e., 1.89% and 0.31% of the total motion range respectively.

4.3 Discussion

In the first experiment, the actuator is designed to track 17.6um P-P stationary sinusoids. The PID and $\mathcal{L}_1$ controller can track the desired trajectory with acceptable tracking error. In the second experiment, the desired trajectory is a sinusoidal path with decreasing amplitude. Tracking errors produced by PID and $\mathcal{L}_1$ controller are summarized and listed in Table1. By comparison, it is clearly that the performance of $\mathcal{L}_1$ is much better for both scenarios.

Table 1: Performance comparison between PID and $\mathcal{L}_1$

		Experiment 1		Experiment 2	
		um	%	um	%
PID	PP	1.438	6.53%	1.315	5.97%
	RMS	0.492	2.23%	0. 3768	1.71%
$\mathcal{L}_1$	PP	0.4553	2.06%	0.4178	1.89%
	RMS	0.1071	0.48%	0.0689	0.31%

Therefore, the $\mathcal{L}_1$ adaptive control algorithm is promising in offsetting the uncertain hysteresis nonlinearity within piezoelectric actuators without the requirement of explicitly modeling it. The theoretical result is validated by our experimental outcomes.

It is also noticeable that the tracking performance of the designed controller is highly limited by the resolution of the displacement sensor and data acquisition card. With the help of hardware with higher resolution and more computing power, more accurate motion tracking performance can be attained even with the $\mathcal{L}_1$ controller proposed in this work.

5. CONCLUSIONS

Nonlinearities existing in piezoelectric actuators highly limit their effectiveness in various applications. Hysteresis is very challenging to compensate due to its varying behavior and difficulties to achieve an accurate model. In this paper, a model-free $\mathcal{L}_1$ adaptive control mechanism is proposed to tackle hysteresis within piezoelectric actuators. Real-time sinusoidal motion tracking experiments verify that the proposed controller can improve the tracking performance in comparison to PID counterpart in terms of peak-to-peak and RMS tracking error. Furthermore, the implementation of the $\mathcal{L}_1$ adaptive controller does not require any *a priori* information of the actuator system. Therefore, it can be readily extended to other applications.

ACKNOWLEDGEMENT

This work is supported by National Natural Science Foundation (NNSF) of China under Grant 61104008, National High Technology Research and Development Program of China (863) under Grant 2012AA062201, and Research Fund for the Doctoral Program of Higher Education of China under Grant 20110101120063.

REFERENCES

Banning, de Koning, Willem L., Adriaens, J.M.T.A, & K.Koops, Richard (2001) "State-space analysis and identification for a class of hysteretic systems". *Automatica*, vol.37, pp.1883-1892.

Cao, C., and Hovakimyan, N. (2006). Design and analysis of a novel L1 adaptive controller, Part I: Control signal and asymptotic stability. *American Control Conference*, 2006 (pp. 3397-3402). IEEE.

Chen, Y., Qiu, J., Palacios, J., and Smith, E. C. (2013). Tracking control of piezoelectric stack actuator using modified Prandtl–Ishlinskii model. *Journal of Intelligent Material Systems and Structures*, 24(6), 753-760.

de Koning, W. L., Adriaens, H., and Banning, R. (1998). Physical modeling of piezoelectric actuators for control purposes. *In Atelier international IFAC sur motion control*, pp. 39-44.

Devasia S., and Moheimani S.O.Reza. (2007). "A Survey of Control Issues in Nanopositioning". *IEEE Transactions on Control Systems Technology*, vol.15, no.5, pp.802-823.

Fan X., Ralph C.Smith. (2008). "$\mathcal{L}_1$ Adaptive Control of Hysteresis in Smart Materials". *Proc. of SPIE*, vol.6926, 69260G.

Fleming, A. J., and Moheimani, S. R. (2005). A grounded-load charge amplifier for reducing hysteresis in piezoelectric tube scanners. *Review of Scientific Instruments*, 76(7), 073707-073707.

Ge, P., & Jouaneh, M. (1996). Tracking control of a piezoceramic actuator. *IEEE Transactions on Control Systems Technology*, vol.4, no.3, pp.209-216.

Li, C., and Tan, Y. (2004). A neural networks model for hysteresis nonlinearity. *Sensors and Actuators A: Physical*, 112(1), 49-54.

Li, Y., and Xu, Q. (2010). Adaptive sliding mode control with perturbation estimation and PID sliding surface for motion tracking of a piezo-driven micromanipulator. *IEEE Transactions on Control Systems Technology*, vol.18, no.4, pp.798-810.

Physik Instrumente. (2009), *Piezo Nano positioning Inspirations*. ,2-185.

Song, G., Zhao, J., Zhou, X., and De Abreu-García, J. A. (2005). "Tracking control of a piezoceramic actuator with hysteresis compensation using inverse Preisach model". *Mechatronics, IEEE/ASME Transactions on*, 10(2), 198-209.

Zou, X., Luo, J., and Cao, C. (2013), Adaptive control for uncertain hysteretic systems. *ASME J. Dyn. Sys., Meas., Control*; 136 (1), 011011-011011-7.